Peroxyacetyl Nitrate and Ozone Enhancement at Taehwa Research Forest under the Influence of Seoul Metropolitan Area

Article *in* Aerosol and Air Quality Research · September 2018

DOI: 10.4209/aaqr.2017.11.0451

CITATIONS
0

READS
270

8 authors, including:

Jihyun Han
Korea Environment Institute
18 PUBLICATIONS **140** CITATIONS
SEE PROFILE

Alex B. Guenther
University of California, Irvine
648 PUBLICATIONS **36,555** CITATIONS
SEE PROFILE

Aerosol and Air Quality Research, 18: 2262–2273, 2018

ISSN: 1680-8584 print / 2071-1409 online
doi: 10.4209/aaqr.2017.11.0451

Peroxyacetyl Nitrate and Ozone Enhancement at Taehwa Research Forest under the Influence of Seoul Metropolitan Area

Junsu Gil[1], Meehye Lee[1,2*], Jihyun Han[1,3], Joo-Ae Kim[1], Saewung Kim[4], Alex Guenther[4], Hyunseok Kim[5,6], Soyoung Kim[7], Sanguk Lee[8], Danbi Kim[8]

[1] *Department of Earth and Environmental Science, Korea University, Seoul 02841, Korea*
[2] *Green School, Korea University, Seoul 02841 Korea*
[3] *Korea Environment Institute, Sejong 30147, Korea*
[4] *Department of Earth System Science, University of California, Irvine, CA 92697, USA*
[5] *Department of Forest Sciences, Seoul National University, Seoul 08826, Korea*
[6] *Research Institute for Agriculture and Life Sciences, Seoul National University, Seoul 08826, Korea*
[7] *Han River Basin Environmental Office, Gyeonggi-do 12902, Korea*
[8] *National Institute of Environmental Research, Incheon 22689, Korea*

ABSTRACT

Peroxyacetyl nitrate (PAN) is produced by photochemical oxidation reactions with abundant NO_x and volatile organic compounds (VOCs); therefore, it is considered as a photochemical pollution indicator. In this study, PAN, O_3, and their precursors were measured at three heights (5.4, 23, and 40.5 m) on a 41-m tower in Taehwa Research Forest (TRF) near the Seoul Metropolitan Area (SMA) from August 25 to September 9, 2011. The PAN was determined every 2 minutes using gas chromatography with luminol chemiluminescence detection (GC-LCD). All reactive gases were measured for 15 minutes at each height. The mean and maximum PAN concentrations were 0.3 and 3.1 ppbv, respectively. The mean and maximum O_3 concentrations were 13.1 and 79.8 ppbv, respectively. The average NO_x concentration was 6.57 ppbv. At the TRF, PAN and O_3 concentrations were well correlated (r = 0.8) and greatly elevated when the air mass was affected by urban outflows from the SMA, which was clearly demonstrated by an increase in NO_2. These high NO_2 concentrations were observed along with a shift in wind direction at 17:00 (KST) and resulted in the maximum observed values of PAN and O_3 in the present study. In addition, the concentration enhancement was more pronounced for PAN and at heights above the canopy. These results highlight PAN as a robust tracer indicating urban impacts at peri-urban forest sites.

Keywords: Peroxyacetyl nitrate (PAN); Ozone (O_3); Peri-urban forest; Taehwa Research Forest; Seoul Metropolitan Area.

INTRODUCTION

Ozone (O_3) is primarily recycled through photochemical reactions of NO_x and volatile organic compounds (VOCs) in urban air, during which peroxyacetyl nitrate (PAN) is formed as a byproduct (Taylor, 1969; Brich *et al.*, 1984; Jenkin and Clemitshaw, 2000; Teklemariam and Sparks, 2004; Braslavsky and Rubin, 2011; Matsumoto, 2014; Tuncay *et al.*, 2015). As PAN is produced in the presence of NO_2 and peroxyacetyl (PA) radical which is an oxidation product of VOCs and destroyed mainly by thermal decomposition, its concentration shows greater sensitivity to precursor levels than O_3 (Nielsen *et al.*, 1981; Tsalkani *et al.*, 1987; Schrimpf *et al.*, 1995; Xu *et al.*, 2015; Han *et al.*, 2017). Thus, PAN is considered a suitable photochemical pollution indicator and has been extensively investigated to understand the driving mechanisms of O_3 pollution in large urban areas (Finlayson-Pitts and Pitts Jr, 1986; Gaffney *et al.*, 1989; Gaffney *et al.*, 1999).

In this context, PAN has been measured mostly in megacities, including Los Angeles, since the 1970s (Lonneman *et al.*, 1976; Tuazon *et al.*, 1981; Grosjean, 1982). During the 2000s, PAN measurements with concentrations ranging from 0.8 to 30 ppbv were reported for Mexico City, Seoul, Beijing and other major Chinese cities (Table 1). On the west coast of the United States, PAN has been paid much attention in association with long-range transport of PAN-enriched Asian outflow and has served as a reliable indicator of its influence (Jaffe *et al.*, 1999; Hudman *et al.*, 2004; Briggs *et al.*, 2016; Baylon *et al.*, 2017). In these studies, PAN concentrations ranged from 0.02 to 0.2 ppbv, much lower than the concentrations observed in northeastern Asia under the influence of continental outflows (Zhang *et*

* Correspond author.
E-mail address: meehye@korea.ac.kr

Table 1. Mean and maximum concentrations of PAN and O_3 from previous studies that were conducted during a similar time interval to the present study.

Site	Type (Altitude, m asl)	Time	PAN (Mean/Max, ppbv)	O_3 (Mean/Max, ppbv)	Reference
This study	Mixed forest (200)	Aug–Sep 2011	0.31/3.13	13.1/79.8	
California, US	Ponderosa pine plantation (1315)	Aug–Oct 2007	0.45/1.47	57/83	(LaFranchi *et al.*, 2009)
Mexico City, Mexico	Urban	Feb–Mar 1997	-/over 30	-/250	(Gaffney *et al.*, 1999)
Hyytiälä, Finland	Boreal forest (181)	July–Aug 2010	-/0.8	-/-	(Phillips *et al.*, 2013)
Michigan, US	Aspen forest (31.5 tower)	July–Aug 1998	0.092/0.94	-/-	(Thornberry *et al.*, 2001)
Oregon, US	Mountain (2763)	Apr 2008–May 2010	0.117/0.53	53/-	(Fischer *et al.*, 2011)
Pearl River Delta, China	Rural	Jul 2006	1.32/3.90	-/-	(Wang *et al.*, 2010)
Writtle, UK	Rural	Aug 2003 (Heatwave period), Day	0.24/0.65	-/150	(Lee *et al.*, 2006)
		Aug 2003 (Heatwave period), Night	0.14/0.43	-/112	
Lanzhou & Mt. Waliguan, China	Mountain near urban (1631)	June–July 2006, Day	0.76/9.13	53/161	(Zhang *et al.*, 2009)
	Qinghai-Tietan Plateau (3816)	July–Aug 2006, Night	0.44/1.40	59/91	
Seoul, Korea	Urban	May–June 2004, 2005	0.80/10.4	31/141	(Lee *et al.*, 2008)
Baengyeong Island, Korea	Regional background	Aug 2010–March 2011	0.38/-	34/-	(Lee *et al.*, 2012)

al., 2017).

The method of measuring PAN was first introduced by Darley (Darley *et al.*, 1963), who used gas chromatography (GC) coupled with electron capture detection (ECD). GC with luminol-based chemiluminescence (GC-LCD) detection was constructed using a packed column (Blanchard *et al.*, 1990) and later improved by employing a short capillary column, which enabled fast and sensitive measurements with high time-resolutions and low detection limits (Gaffney *et al.*, 1998). Recently, the thermal dissociation-chemical ionization mass spectrometry (TD-CIMS) technique has become commercially available (Slusher *et al.*, 2004).

As a precursors of PAN, NO_x is mainly emitted from vehicles in urban areas, whereas the PA radical is produced from acetaldehyde, methylglyoxal, and acetone that are directly emitted or photochemically generated by oxidation process of anthropogenic VOCs (AVCOs) and biogenic VOCs (BVOCs) (Singh and Hanst, 1981; Roelofs *et al.*, 1997; Choi, 2003; Calfapietra *et al.*, 2013; Fischer *et al.*, 2014; Carslaw *et al.*, 2016; Sobanski *et al.*, 2017). Although AVOCs are dominant in urban areas, BVOCs are more abundant on the global scale and their emissions are estimated at 760–1150 Tg C $year^{-1}$ which comprises about 90% of total VOC emissions (Guenther *et al.*, 2012; Sindelarova *et al.*, 2014). Therefore, there is significant PAN production in forests proximal to urban areas due to the abundant VOCs and NO_x (Sobanski *et al.*, 2017).

Since BVOCs were first pointed out as the precursors of "blue haze" in mountainous regions (Went, 1960), researchers have demonstrated their role in tropospheric photochemistry that isoprene, the most abundant species of BVOC, has been intimately involved in southern U.S. ozone formation (Chameides *et al.*, 1988). It is quite recent in East Asia that BVOCs have been investigated in the view of its role in atmospheric chemistry and have been measured in Beijing (Ran *et al.*, 2011), Kyoto (Bao *et al.*, 2010), and Shanghai (Geng *et al.*, 2011). In the vicinity of California, secondary organic aerosols become highly enhanced when urban plumes are mixed with biogenic emissions (Shilling *et al.*, 2013). Consequently, this study emphasizes the importance of measurements in forests, which are major sources of BVOCs.

In South Korea, forest areas consist of coniferous trees (42%) and deciduous trees (26%) comprises 65% of the country (KFS, 2013). The percentage of total forest area is even larger in major cities with 72% on average, including Seoul Metropolitan Area (SMA). In these major cities of Korea, O_3 concentration has increased since 2005 (Ghim, 2012) and a $PM_{2.5}$ mass concentration was implemented in 2015 as a national environmental standard. Previous studies have shown that O_3 formation shows more sensitivity to VOCs than NO_x in SMA (Han *et al.*, 2013). Thus, with the growing demand for improved air quality, the impact of BVOCs on O_3, PAN, and secondary aerosols formation needs to be thoroughly understood (Ran *et al.*, 2011). Within this context, the National Institute of Environmental Research (NIER) initiated research to investigate the effect of BVOCs on air quality and established a measurement station with a tall tower at Taehwa Research Forest (TRF). In 2016, the TRF served as a ground platform for the

Korea-US Air Quality (KORUS-AQ) and Megacity Air Quality Study-Seoul (MAPS-Seoul) campaigns. The results regarding BVOCs and O_3 conducted at the TRF since 2011 can be found in other publications (Kim *et al.*, 2013; Kim, 2014; Kim *et al.*, 2015a; Kim *et al.*, 2015b).

In this study, the temporal and vertical distributions of PAN were thoroughly examined to understand how the urban emissions of NO_x affect PAN and O_3 concentrations when it is mixed with biogenic precursors in a peri-urban forest.

EXPERIMENT

The measurements of PAN and other trace gases, including O_3, NO_x, CO, and SO_2, were conducted at TRF from August 25 to September 9, 2011. The TRF constitutes approximately 800 ha of afforested area that was established by education and research of the College of Agriculture and Life Sciences at Seoul National University. The TRF is located ~25 km southeast of Seoul and its satellite cities lie on the west (Fig. 1). On the east side of the forest, the Central Highway extends to the north and south. The observation facilities including a 41-m walkup tower and laboratory are located 165 m above the sea level (37.18°N, 127.19°E) in a planted Korean pine (*Pinus koraiensis Siebold et Zucc.*) coniferous forest (299 ha). The surrounding region (476 ha) is a natural deciduous forest such as Murray (*Quercus serrata Murray*) and Blume (*Quercus aliena Blume*). The tower is equipped with sampling inlets at heights of 5.4, 23, and 40.5 m and has meteorological sensors at 5.4 and 40.5 m. The canopy height of TRF is approximately 21 m above the ground surface.

The air was pulled down to the manifold through PFA tubing (OD of 6.35 mm, ID of 3.96 mm) at 10 L min^{-1} at the three heights of the tower. At each height, air was sampled for 15 minutes, producing hourly vertical measurement profile. From the manifold, air was distributed for PAN, O_3, NO_x, CO, and SO_2 measurements. PAN was measured every 2 minutes using a fast GC-LCD system (Marley *et al.*, 2004; Lee *et al.*, 2008). The sampled air was introduced to the 6-port valve (Cheminert C22, Valco Instruments, TX, USA) at 100 mL min^{-1} and injected into the capillary column (DB-1, J&W Scientific, CA, USA) through a 2 cm^3 sample loop by nitrogen gas at 30 mL min^{-1}. The air flow was controlled by a mass flow controller (Alicat Scientific Inc., AZ, USA). Luminol solution constantly flowed into the reaction cell at 0.6 mL min^{-1}, where the chemiluminescence signal was detected by a photon counter (HC135-01, Hamamatsu, NJ, USA). The PAN standard solution was synthesized by peracetic acid with *n*-tridecane at temperatures below 20°C (Gaffney *et al.*, 1998). The detailed calibration procedure can be found elsewhere (Han *et al.*, 2017). The nominal PAN detection limit was 0.1 ppbv (Lee *et al.*, 2008).

Other trace gases, such as O_3, NO_x, CO, and SO_2, were measured every minute by a conventional monitoring instrument (49i, 42i, 48i, and 43i, Thermo Electron Incorporation, MA, USA). For discussion, all measurements data were averaged for 2 minutes according the PAN measurement resolution. The temperature and relative humidity (RH) measurements are available from August 29 onwards at TRF.

The backward trajectories of air masses were calculated using the Hybrid Single Particle Lagrangian Integrated Trajectory (HYSPLIT) model with Global Data Assimilation System (GDAS) data from the National Oceanic and Atmospheric Administration (NOAA), in conjunction with Trajstat software (Wang, 2014).

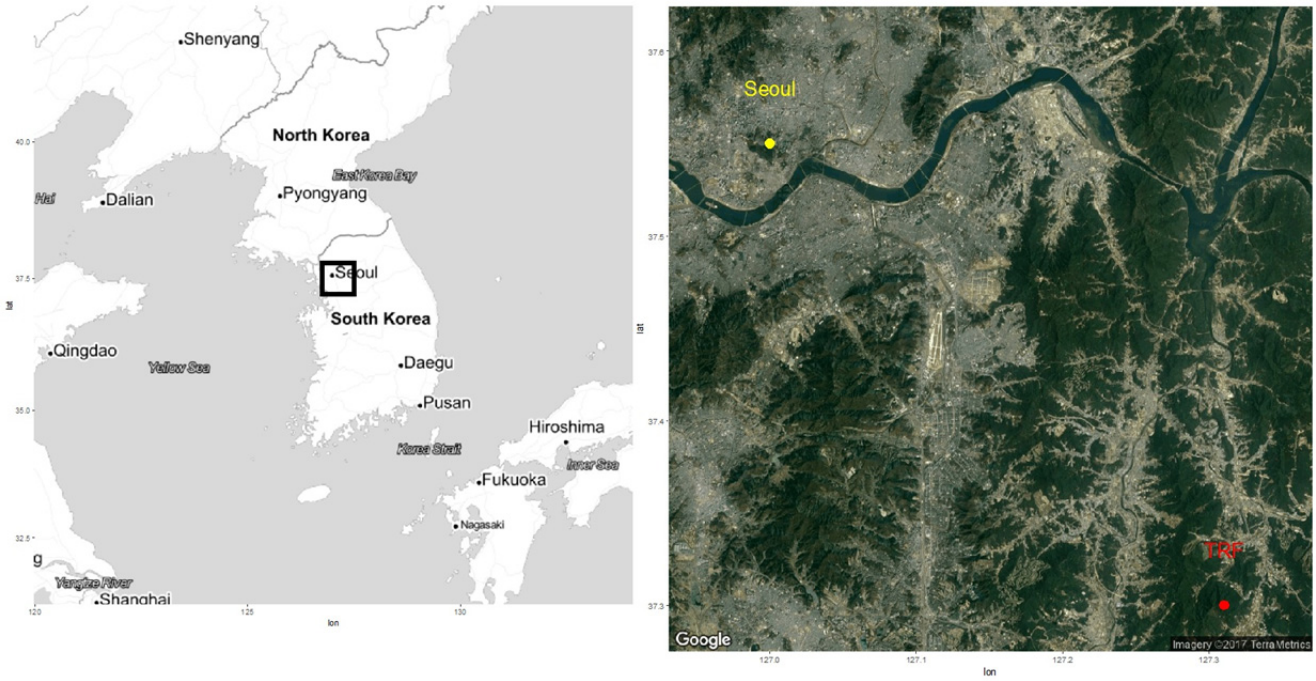

Fig. 1. Study regions, including the Korean Peninsula and Seoul Metropolitan Area (SMA). The region inside the black box is enlarged and shows the location of the Taehwa Research Forest (TRF) (from Google Earth).

RESULTS AND DISCUSSION

Characteristic Distribution of PAN and Other Trace Gases

During the experiment, temperature gradually decreased from August to September (Fig. 2). During the first four days, without meteorological measurements from the TRF, the daily maximum temperatures were above 30°C in Seoul and nearby cities. Although the experiment period was characterized by low levels of primary pollutants (e.g., SO_2, NO_x, and CO) in Korea under the influence of maritime air (MOE, 2011), trace gases show considerable variations and their highest concentrations are commensurate to SMA levels.

Throughout the experiment, PAN concentration had a mean of 0.3 ppbv and reached a maximum of 3.13 ppbv (Table 1). The mean and maximum concentrations of all measurements are listed in Table 1. The mean PAN concentration in this study is comparable to concentrations observed at forest sites (0.1–0.45 pbv), but lower than those at rural sites (0.43–0.76 ppbv) (Table 2). In contrast, the maximum PAN concentration in this study is significantly higher than concentrations measured at other forest sites (0.53–1.47 ppbv) and comparable to those at rural sites (3.90 ppbv). O_3 concentration averaged 13.7 ppbv, which is considerably lower than measurement in forest regions (53–57 ppbv) and background site of the study region (34 ppbv). The maximum O_3 (79.8 ppbv) was also lower than those of other sites (83–161 ppbv). The CO and SO_2 levels of the TRF were lower than those of the SMA and comparable to those of background sites of the study region (MOE, 2011). The mean concentration of NO_x was much lower than SMA, but the highest concentrations were higher than those typically observed in forests (Kim, 2014).

The temporal variations of PAN and O_3 are shown in Fig. 2 with the NO_x and CO concentration. Apparently, the experiment period falls into two high- and two low-concentration episodes from the variations of these trace gases: August 25–28, August 29–September 2, September 3–4, September 5–9. In the averaged diurnal variations, PAN and O_3 concentrations reached maximum at 15:00 (local time) (Fig. 3(a)). Although the maximum NO_x concentration was identified at 09:00, diurnal variation was unclear throughout the day and the amplitude of averaged diurnal change was less than 3 ppbv from the 5 ppbv baseline concentration.

A polar plot is known to be useful tool to investigate source characteristics of air pollutants (Grange *et al.*, 2016). The polar plot incorporated with wind measurements illustrates that NO_x is affected by nearby sources, such as emissions from the highway in the east and the urban areas in the west (Fig. 3(b)). In comparison, the highest PAN and O_3 concentrations are associated with relatively weak northwesterly and strong northerly winds, respectively.

The vertical distributions of PAN, O_3, and NO_x concentrations were compared on a frequency histogram overlaid with the three heights (5, 23, and 40.5 m) (Fig. 3(c)). For these three species, the highest concentrations were mostly observed above canopy (i.e., 23 and 40.5 m). These results demonstrate that the TRF represents a peri-urban forest where nearby urban emissions are mixed with biogenic emissions from vegetation (Ham *et al.*, 2016). The characteristic distributions of PAN, O_3, and NO_x are further discussed in the following sections.

Controlling Factors of PAN and O_3 Levels

In this study, PAN is strongly correlated with O_3 (Pearson's correlation coefficient, $r = 0.8$), and there is also a strong positive relationship between the daily maximum concentrations of PAN and O_3 ($r = 0.78$), usually observed in urban areas (Lee *et al.*, 2008; Zhang *et al.*, 2009). Daily maximum PAN and O_3 concentrations have also been reported to correlate strongly with daily maximum temperature (Wunderli and Gehrig, 1991), implying that temperature is an important factor in the formation of these two species. In this study, the daily maximum PAN and O_3 concentrations did not always proportionally increase with the daily maximum temperature (Fig. 4). This inconsistency is because PAN and O_3 concentrations showed a sudden drop with temperature between September 3 and 4, along with relative humidity (Fig. 2). The time series of all measurements also reveals that PAN, O_3, and primary pollutants level changed every 2–5 days. As meteorological changes are dynamic in northeast Asia, the air mass pathways were examined as a potential control factor affecting atmospheric processes and precursor levels at the TRF.

The backward trajectories calculated using the HYSPLIT model illustrate that air mass changes occurred frequently during the 16-day experiment (Fig. 5). At the beginning of the experiment, enhanced NO_2 and O_3 concentrations were associated with air coming from the East Sea through southern South Korea. As stagnant conditions developed, the air mass that lingered over the SMA arrived at the TRF, leading to the highest PAN and O_3 concentrations in the end of August. As air moved northeast rapidly from the East Sea, all reactive gas concentrations dropped down to the lowest observed levels with a decrease in relative humidity from September 3 to 4. PAN and O_3 levels were elevated again between September 5 and 7, when the air quickly passed through the SMA and arrived at the TRF. According to these observations, the entire experimental period was divided into four intervals (i.e., P1, P2, P3, and P4), within which the behaviors of PAN and O_3 were examined in detail. The measurement statistics for each period are summarized in Table 3.

PAN and O_3 concentrations were highly elevated in P2 and P4 when the air passed over the SMA. The maximum concentrations of both species were observed in P2 and corresponded with the high NO_2 concentrations and NO_2/NO_x ratios (Fig. 6). For each period, the correlation between O_3 and PAN is presented in Fig. 6(a). In P4, PAN was relatively more elevated than O_3, corresponding to high CO and NO concentrations and a low NO_2/NO_x ratio. The low O_3/PAN ratios in P2 and P4 indicate that PAN was relatively more elevated than O_3 in the presence of urban emission influence at the TRF. It is also noteworthy that the PAN/O_3 ratio was highest during P4, of which urban plumes were likely less aged compared with those of P2, based on their history and chemical signature. In contrast, O_3 concentrations were relatively higher than PAN concentrations during P1,

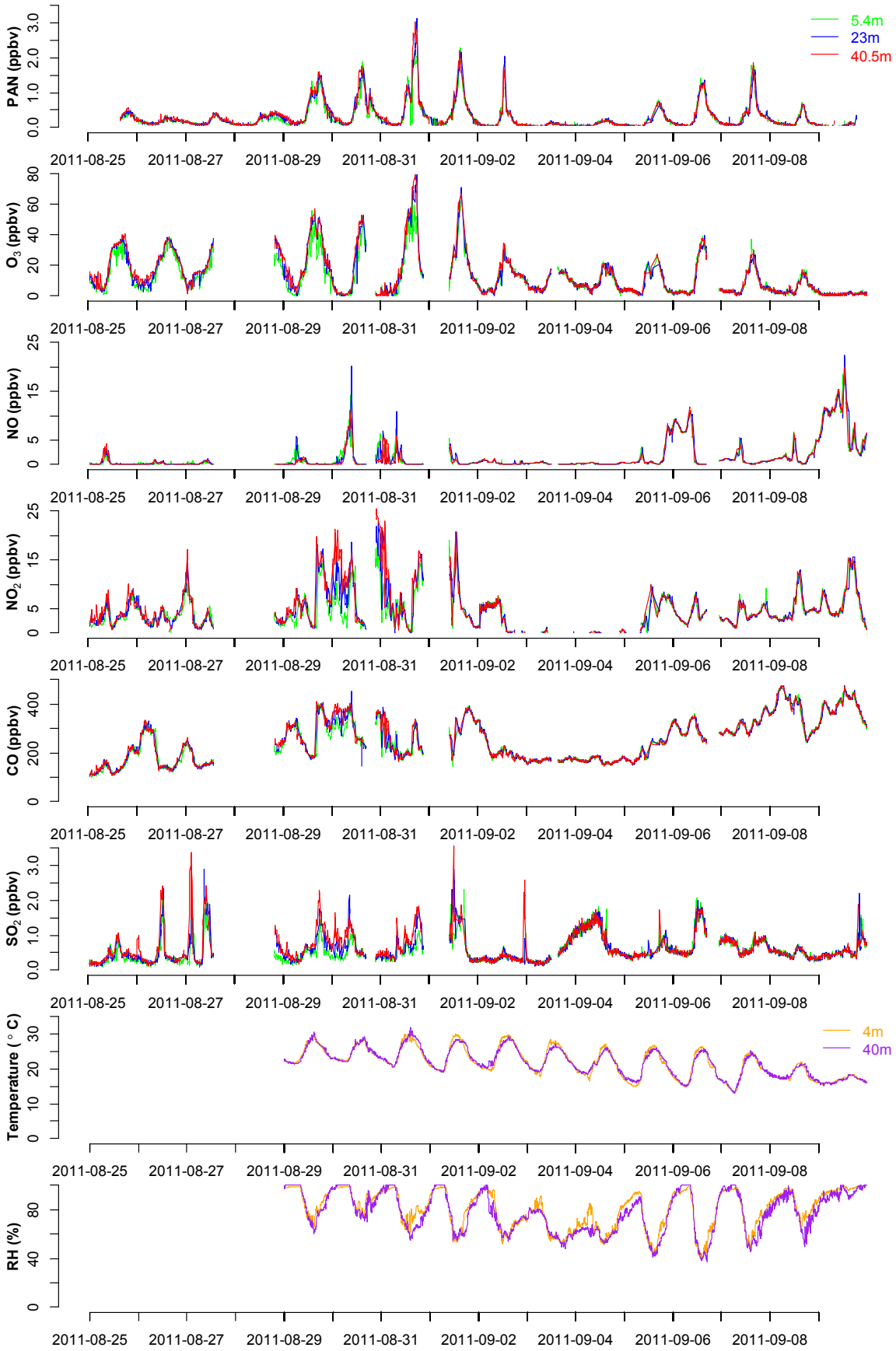

Fig. 2. Temporal variations of measured PAN, O_3, NO, NO_2, CO, and SO_2 concentrations at 5.4, 23, and 40.5 m and temperature and relative humidity measured at 4 and 40 m.

Table 2. Mean and maximum concentrations of all measured species (2-minute data) at each height.

	5.4 m	23 m	40.5 m
PAN (ppbv)	0.29, (2.29)	0.32, (3.13)	0.32, (3.04)
O_3 (ppbv)	12.1, (67.0)	13.6, (79.6)	13.8, (79.8)
NO (ppbv)	1.5, (18.4)	1.6, (22.4)	1.5, (20.0)
NO_2 (ppbv)	4.6, (19.0)	5.1, (22.4)	5.4, (25.4)
CO (ppbv)	251, (473)	255, (475)	256, (475)
SO_2 (ppbv)	0.56, (2.31)	0.62, (2.92)	0.65, (3.58)

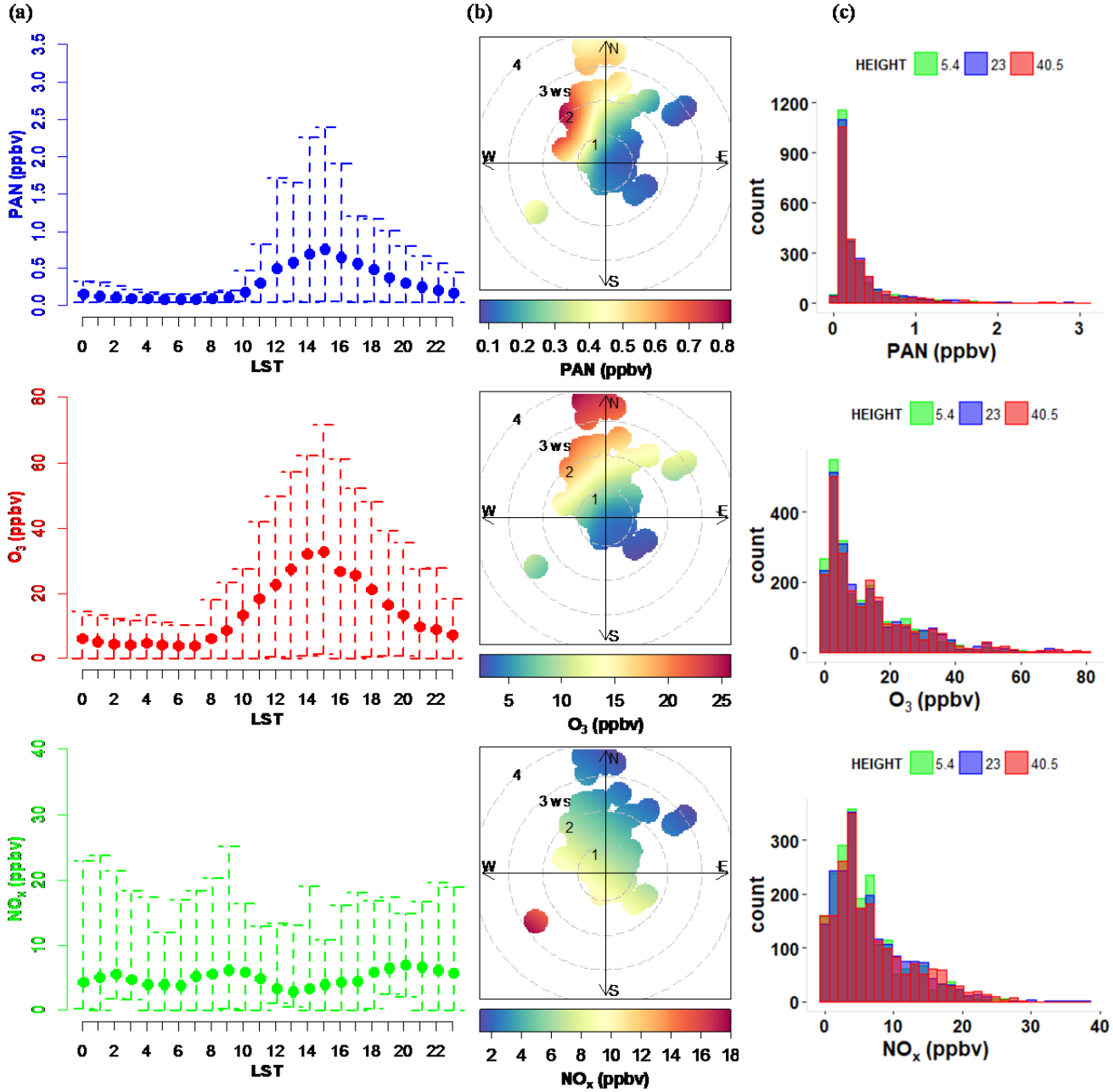

Fig. 3. (a) Diurnal variations and (b) polar plots of PAN, O_3, and NO_x measurements for all three heights. (c) Frequency histogram of PAN, O_3, and NO_x overlaid with the three heights. In (a), the bars and solid circles correspond to the inter quartile ± 1.5 inter-quartile range (IQR) and the median, respectively.

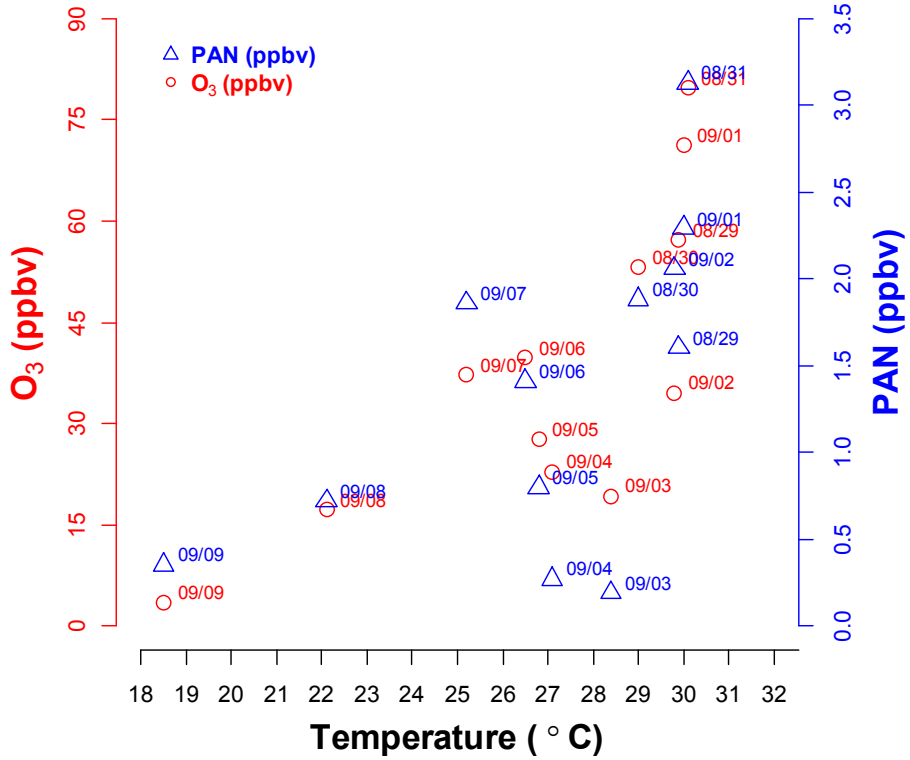

Fig. 4. Daily maximum PAN and O_3 concentrations against daily maximum temperature.

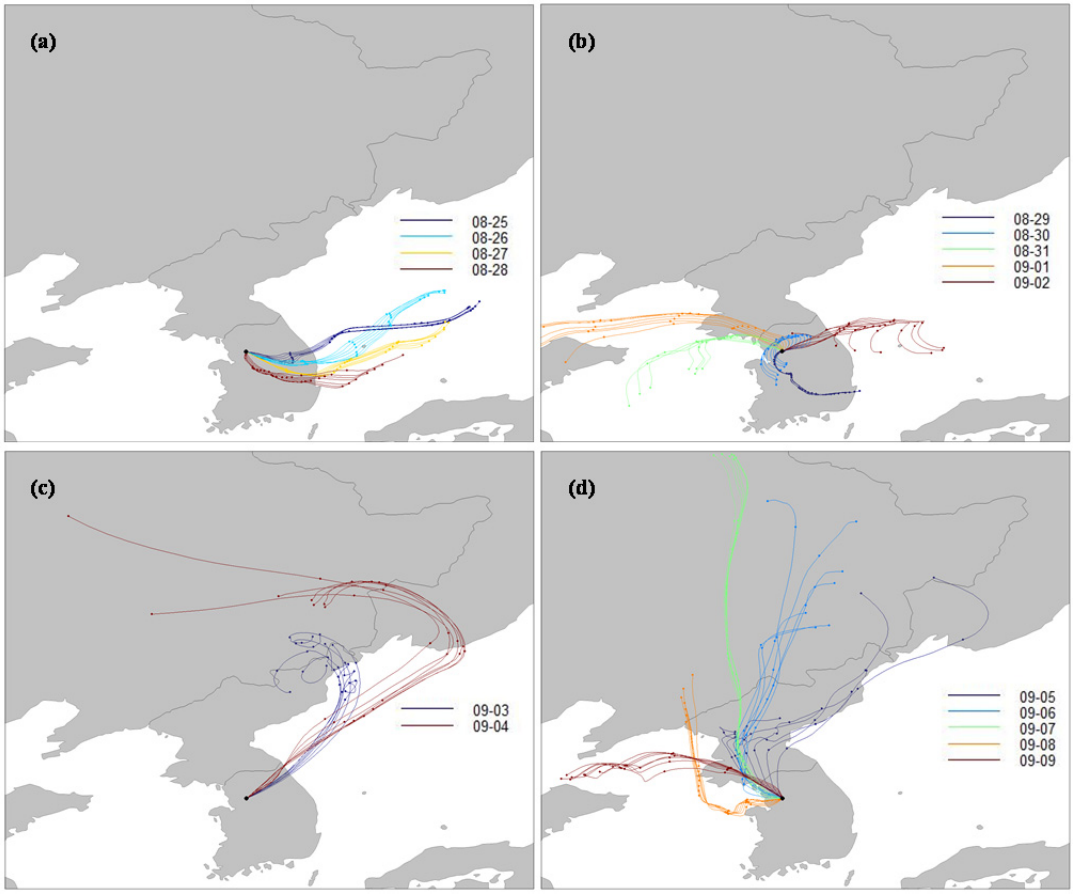

Fig. 5. 48-hour backward trajectories of air masses arrived at 1000 m altitude above the TRF hourly, between 12:00 and 18:00 for the four periods: (a) P1, (b) P2, (c) P3, and (d) P4 as distinguished in Table 3.

Table 3. The entire experiment was separated into four groups, for which the average concentrations of reactive gases are given with the maximum of PAN and O_3.

Date	P1 (8/25–8/28)	P2 (8/29–9/2)	P3 (9/3–9/4)	P4 (9/5–9/9)
O_3 (ppbv)	18.7, (40.9)	18.6, (79.8)	9.0, (22.9)	6.5, (39.8)
PAN (ppbv)	0.20, (0.57)	0.49, (3.13)	0.10, (0.27)	0.28, (1.86)
NO (ppbv)	0.23	0.86	0.20	3.49
NO_2 (ppbv)	3.64	6.59	0.30	4.80
CO (ppbv)	179	267	196	319
NO_2/NO_x	0.94	0.88	0.6	0.58
O_3/PAN	93.5	38.0	89.9	23.2
PAN/NO_2	0.05	0.07	0.33	0.08

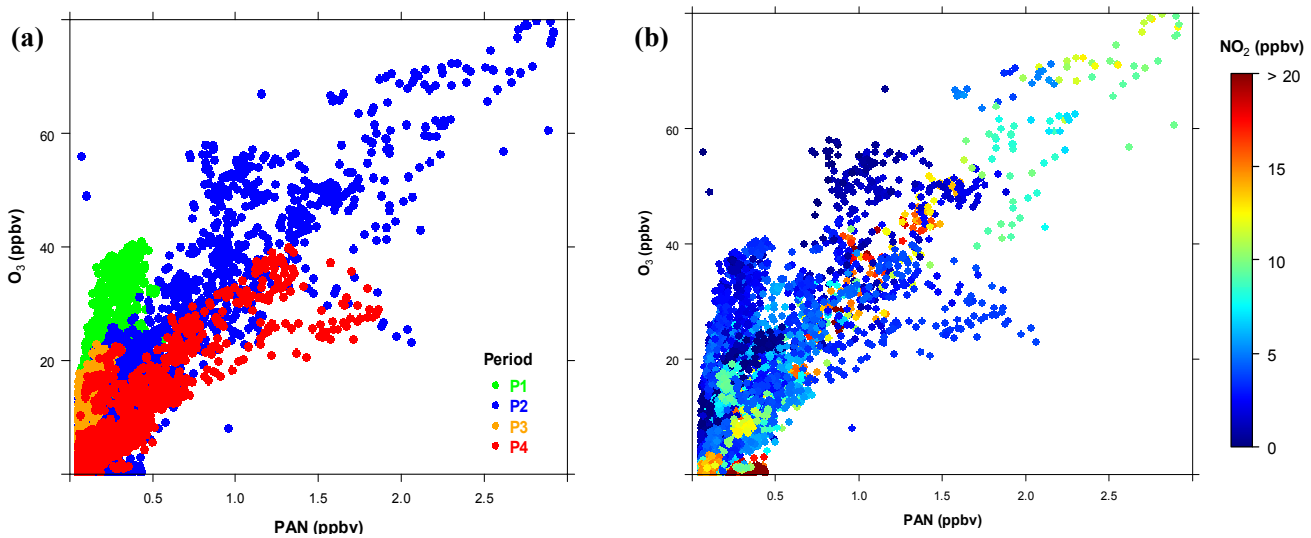

Fig. 6. Correlation between PAN and O_3 concentrations within (a) the four periods and (b) color-coded by NO_2 concentrations.

which had the highest NO_2/NO_x ratios and temperatures (measured nearby).

At the TRF, the measurement results of PAN and O_3 demonstrate that while the O_3 levels are sensitive to temperature and degree of chemical aging, the PAN concentrations are sensitive to NO_x levels, which agrees with the current understanding of tropospheric photochemistry. As a result, PAN concentrations were greatly elevated when the air mass was affected by emissions from the SMA, of which degree of enhancement was largely dependent on meteorological conditions. These results highlight PAN as a robust tracer indicating urban emissions at a peri-urban forest.

Urban Influence on PAN and O_3 Enhancement

The correlation between PAN and O_3 was different in each of the four periods, and the best correlation was observed in P2 (Fig. 6(a)). In P2, PAN and O_3 time-series distributions show the afternoon maximum peak split into two peaks, and more pronounced for PAN than for O_3 (Fig. 2). This was particularly evident on August 31, when the second peak was much larger than the first and concurrent with elevated NO_2. Thus, NO_2 concentration was added to the correlation between PAN and O_3 in Fig. 6(b). In urban air, PAN and O_3 are produced by photochemical reactions and their concentrations usually reach maximum during the afternoon when NO_2 concentrations are lowest (Lee *et al.*, 2008). However, at Jeju Island, a background site in northeast Asia, PAN concentrations were unusually elevated concurrently with NO_2 in continental outflow plumes (Han *et al.*, 2017). Similarly, in this study, the highest concentrations of PAN and O_3 were associated with elevated NO_2 concentrations, particularly during P2. The PAN and O_3 concentrations on August 31, when the PAN and O_3 maximums were observed, are presented with NO_2 concentrations and wind vectors (Fig. 7).

In Fig. 7, high PAN and O_3 concentrations are distinguished by high NO_2 concentrations, and are observed later than 15:00 after the first peak around 13:00 that is associated with low NO_2. PAN and O_3 gradually increased with a decrease in NO_2 until 13:00, and it agrees with the results expected from photochemical reactions in urban atmosphere. After the first peak at 13:00, PAN concentration decreased whereas O_3 concentration remained high. At approximately 15:00, PAN and O_3 concentrations rapidly increased with an increase in NO_2, leading to maximum observed values at 17:00. During this time interval, PAN concentration increased significantly more than O_3, despite no visible differences in PAN and O_3 concentrations among the three heights at the first peak. In contrast, the

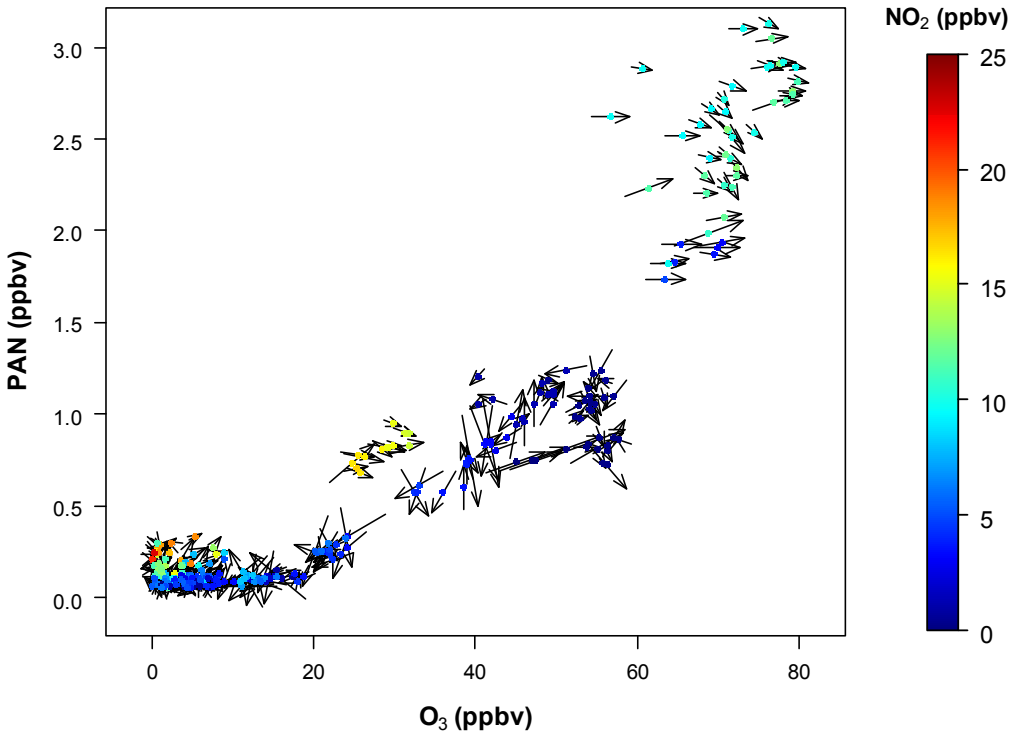

Fig. 7. Variations in PAN and O_3 concentrations along with changes in winds and NO_2 concentrations on August 31th.

late enhancement of these two species was more evident at 23 and 40.5 m (above canopy) than at 5.4 m (below canopy) (Fig. 3(c)). Furthermore, the rapid increases in PAN and O_3 were concurrent with the wind direction change (Fig. 7). In the late afternoon, the northerly/northwesterly winds were consistent. These results demonstrate that the late maximum PAN and O_3 concentrations were affected by urban outflows.

Although VOCs measurements were not available for this experiment, they were measured at the same site between May and August of 2013 (Kim *et al.*, 2015a). During period, isoprene concentration reached a maximum at 17:00, concurrent with the observed PAN and O_3 maximum in this study. Late afternoon isoprene emissions have also been reported in previous work (Apel *et al.*, 2002; Bryan *et al.*, 2012). Although the tower is surrounded by planted pine trees, the TRF is dominated by deciduous trees that are concentrated to the northwest of the tower. Thus, northwesterly winds carry not only urban emissions from the SMA but also isoprene emitted from nearby deciduous trees that was likely to move down to the tower. Isoprene is known as a major VOC that produces PAN on a global scale (Fischer *et al.*, 2014). These facts well agree with the source apportioned for PAN in Fig. 3(b).

As the lifetime of PAN is less than one hour at ~30°C, the observed late afternoon peak in PAN concentration was unlikely because of transport from the SMA. On the other hand, the solar zenith angle was 67° at 17:00, suggesting that in-situ photochemical reactions could not fully account for the elevation of PAN concentrations in the late afternoon. Taking these results into consideration, BVOCs may have played a role in the rapid increase of PAN and O_3 concentrations to the maximum in the late afternoon. With a shift in wind direction, the TRF was under the influence of urban emissions from SMA. On the way to being transported to the tower, the plume passed over the forest region, thereby being mixed with biogenic emissions. Therefore, it is highly likely that PAN was produced from nearby forest upon the influx of urban emissions and moved to the sampling tower. As PAN is sensitive to precursor levels, the PAN increase was instantaneous with increases in NO_2. Although the similar increase of O_3 concentration raised to the maximum at 17:00, the enhancement of the second peak relative to the first peak was much greater for PAN (3.1 vs. 1.5 ppbv) than O_3 (79.6 vs. 56.1 ppbv) (Fig. 7).

CONCLUSIONS

The mean and maximum concentrations of PAN and O_3 were 0.3 ppbv and 3.1 ppbv, and 13.1 ppbv and 79.8 ppbv, respectively. Overall, the two species were strongly correlated (r = 0.8), but their maximum daily concentrations did not always proportionally increase with the temperature. In this study, the PAN and O_3 levels varied considerably with meteorological conditions and were largely dependent on the degree of urban influence. Accordingly, NO_x and CO concentrations ranged from summer background to major Korean city levels with means of 6.6 ppbv and 254 ppbv, respectively.

As the TRF is a peri-urban forest, the PAN and O_3 concentrations there were significantly elevated under the influence of the SMA, resulting in the maximum concentrations of the two species during the experiment. The maximum concentrations were observed in late August,

when the diurnal variations of PAN and O_3 showed clear peaks at 13:00 and 15:00. The later peak was associated with urban outflows from the SMA, characterized by a rapid increase in NO_2 concentration and a change in wind direction. Particularly, the enhancement of PAN was more evident than that of O_3 and occurred more obviously above than below the canopy. Another episode with lower temperatures and higher wind speeds occurred in September, during which the PAN/O_3 ratio reached its maximum in the experiment, with less aged outflow from the SMA than the other periods. When PAN and O_3 concentrations remained low, the O_3/PAN ratio was higher, with a higher NO_2/NO_x ratio at higher temperatures.

The measurements at the TRF demonstrate that O_3 concentrations are more sensitive to temperature and air mass aging, whereas PAN concentrations are more sensitive to NO_x. Thus, the results of this study highlight PAN as a robust indicator of the urban impact on peri-urban forests.

ACKNOWLEDGMENTS

This research was supported by the National Institute of Environmental Research (NIER) and Basic Science Research Program through the National Research Foundation of Korea (NRF) funded by Ministry of Science, Information, and Communications Technology & Future Planning (NRF-2017R1A2B4012143). A part of this study was done for the Master's thesis of Hee-Yeon Shim.

REFERENCES

Apel, E., Riemer, D., Hills, A., Baugh, W., Orlando, J., Faloona, I., Tan, D., Brune, W., Lamb, B. and Westberg, H. (2002). Measurement and interpretation of isoprene fluxes and isoprene, methacrolein, and methyl vinyl ketone mixing ratios at the prophet site during the 1998 intensive. *J. Geophys. Res.* 107: ACH 7-1–ACH 7-15.

Bao, H., Shrestha, K.L., Kondo, A., Kaga, A. and Inoue, Y. (2010). Modeling the influence of biogenic volatile organic compound emissions on ozone concentration during summer season in the Kinki region of Japan. *Atmos. Environ.* 44: 421–431.

Baylon, P., Jaffe, D.A., de Gouw, J. and Warneke, C. (2017). Influence of long-range transport of siberian biomass burning at the Mt. Bachelor observatory during the spring of 2015. *Aerosol Air Qual. Res.* 17: 2751–2761.

Blanchard, P., Shepson, P., So, K., Schiff, H., Bottenheim, J., Gallant, A., Drummond, J. and Wong, P. (1990). A comparison of calibration and measurement techniques for gas chromatographic determination of atmospheric peroxyacetyl nitrate (PAN). *Atmos. Environ.* 24: 2839–2846.

Braslavsky, S.E. and Rubin, M.B. (2011). The history of ozone Part VIII. Photochemical formation of ozone. *Photochem. Photobio. Sci.* 10: 1515–1520.

Brich, K., Penkett, S., Atkins, D., Sandalls, F., Bamber, D., Tuck, A. and Vaughan, G. (1984). Atmospheric measurements of peroxyacetylnitrate (PAN) in rural, south-east England: Seasonal variations winter photochemistry and long-range transport. *Atmos. Environ.* 18: 2691–2702.

Briggs, N.L., Jaffe, D.A., Gao, H., Hee, J.R., Baylon, P.M., Zhang, Q., Zhou, S., Collier, S.C., Sampson, P.D. and Cary, R.A. (2016). Particulate matter, ozone, and nitrogen species in aged wildfire plumes observed at the mount bachelor observatory. *Aerosol Air Qual. Res.* 16: 3075–3087.

Bryan, A., Bertman, S., Carroll, M., Dusanter, S., Edwards, G., Forkel, R., Griffith, S., Guenther, A., Hansen, R. and Helmig, D. (2012). In-canopy gas-phase chemistry during cabinex 2009: Sensitivity of a 1-d canopy model to vertical mixing and isoprene chemistry. *Atmos. Chem. Phys.* 12: 8829–8849.

Calfapietra, C., Fares, S., Manes, F., Morani, A., Sgrigna, G. and Loreto, F. (2013). Role of Biogenic Volatile Organic Compounds (BVOC) emitted by urban trees on ozone concentration in cities: A review. *Environ. Pollut.* 183: 71–80.

Carslaw, D.C., Murrells, T.P., Andersson, J. and Keenan, M. (2016). Have vehicle emissions of primary NO_2 peaked? *Faraday discussions* 189: 439–454.

Chameides, W., Lindsay, R., Richardson, J. and Kiang, C. (1988). The role of biogenic hydrocarbons in urban photochemical smog: Atlanta as a case study. *Science* 241: 1473–1475.

Choi, W.S. (2003). *Photochemical processes in Seoul and Incheon, Korea and Yanji, China based on observations of NO, NO_2, NO_y, O_3, PAN, CO, and J(NO_2)*, Master's thesis, Seoul National University, Korea.

Darley, E.F., Kettner, K.A. and Stephens, E.R. (1963). Analysis of peroxyacyl nitrates by gas chromatography with electron capture detection. *Anal. Chem.* 35: 589–591.

Finlayson-Pitts, B.J. and Pitts, J.N. Jr. (1986). *Atmospheric chemistry. Fundamentals and experimental techniques*. Wiley, New York.

Fischer, E., Jacob, D.J., Yantosca, R.M., Sulprizio, M.P., Millet, D., Mao, J., Paulot, F., Singh, H., Roiger, A. and Ries, L. (2014). Atmospheric peroxyacetyl nitrate (PAN): A global budget and source attribution. *Atmos. Chem. Phys.* 14: 2679–2698.

Fischer, E., Jaffe, D. and Weatherhead, E. (2011). Free tropospheric peroxyacetyl nitrate (PAN) and ozone at Mount Bachelor: Potential causes of variability and timescale for trend detection. *Atmos. Chem. Phys.* 11: 5641–5654.

Gaffney, J., Bornick, R., Chen, Y.H. and Marley, N. (1998). Capillary gas chromatographic analysis of nitrogen dioxide and pans with luminol chemiluminescent detection. *Atmos. Environ.* 32: 1445–1454.

Gaffney, J., Marley, N., Cunningham, M. and Doskey, P. (1999). Measurements of peroxyacyl nitrates (PANS) in Mexico City: implications for megacity air quality impacts on regional scales. *Atmos. Environ.* 33: 5003–5012.

Gaffney, J.S., Marley, N.A. and Prestbo, E.W. (1989). Peroxyacyl nitrates (PANS): Their physical and chemical properties, In *Air pollution*, Springer, pp. 1–38.

Geng, F., Tie, X., Guenther, A., Li, G., Cao, J. and Harley, P. (2011). Effect of isoprene emissions from major forests

on ozone formation in the city of Shanghai, China. *Atmos. Chem. Phys.* 11: 10449–10459.

Ghim, Y.S. (2012). Proposal for air quality improvement and green growth in the seoul metropolitan area of the 21st century. *J. Korean Soc. Atmos. Environ.* 28: 109–118.

Grange, S.K., Lewis, A.C. and Carslaw, D.C. (2016). Source apportionment advances using polar plots of bivariate correlation and regression statistics. *Atmos. Environ.* 145: 128–134.

Grosjean, D. (1982). *Critical evaluation and comparison of measurement methods for nitrogenous compounds in the atmosphere*. Final report, Environmental Research and Technology, Inc., Westlake Village, CA (USA).

Guenther, A., Jiang, X., Heald, C., Sakulyanontvittaya, T., Duhl, T., Emmons, L. and Wang, X. (2012). The Model of Emissions of Gases and Aerosols from Nature version 2.1 (MEGAN2.1): An extended and updated framework for modeling biogenic emissions. *Geosci. Model Dev*. 5: 1471–1492.

Han, J., Kim, H., Lee, M., Kim, S. and Kim, S. (2013). Photochemical air pollution of Seoul in the last three decades. *J. Korean Soc. Atmos. Environ.* 29: 390–406.

Ham, J., Lee, M., Kim, H., Park, H., Cho, G. and Park, J. (2016). Variation of OC and EC in $PM_{2.5}$ at Mt. Taehwa. *J. Korean Soc. Atmos. Environ.* 32: 21–31.

Han, J., Lee, M., Shang, X., Lee, G. and Emmons, L.K. (2017). Decoupling peroxyacetyl nitrate from ozone in Chinese outflows observed at Gosan Climate Observatory. *Atmos. Chem. Phys.* 17: 10619–10631.

Hudman, R., Jacob, D.J., Cooper, O., Evans, M., Heald, C., Park, R., Fehsenfeld, F., Flocke, F., Holloway, J. and Hübler, G. (2004). Ozone production in transpacific Asian pollution plumes and implications for ozone air quality in California. *J. Geophys. Res.* 109: D23S10,.

Jaffe, D., Anderson, T., Covert, D., Kotchenruther, R., Trost, B., Danielson, J., Simpson, W., Berntsen, T., Karlsdottir, S. and Blake, D. (1999). Transport of asian air pollution to north America. *Geophys. Res. Lett.* 26: 711–714.

Jenkin, M.E. and Clemitshaw, K.C. (2000). Ozone and other secondary photochemical pollutants: Chemical processes governing their formation in the planetary boundary layer. *Atmos. Environ.* 34: 2499–2527.

KFS (2013). *Korean forests at a glance 2013*, Service, K.F. (Ed.), Korea Forest Service, pp. 1–66.

Kim, D.S. (2014). Practical use of flux gradient similarity theory for forest soil NO flux at Mt. Taewha. *J Korean Soc. Atmos. Environ.* 30: 531–537.

Kim, H., Lee, M., Kim, S., Guenther, A., Park, J., Cho, G. and Kim, H.S. (2015a). Measurements of isoprene and monoterpenes at Mt. Taehwa and estimation of their emissions. *Korean J. Agric. For. Meteorol.* 17: 217–226.

Kim, S., Park, H., Hong, Y., Han, J., Son, J. and Park, J. (2013). Study on the estimation between CO_2 flux in tree and atmosphere. *Clim. Change Res.* 4: 305–316.

Kim, S., Kim, S.Y., Lee, M., Shim, H., Wolfe, G., Guenther, A.B., He, A., Hong, Y. and Han, J. (2015b). Impact of isoprene and HONO chemistry on ozone and OVOC formation in a semirural South Korean forest. *Atmos. Chem. Phys.* 15: 4357–4371.

LaFranchi, B., Wolfe, G., Thornton, J., Harrold, S., Browne, E., Min, K., Wooldridge, P., Gilman, J., Kuster, W. and Goldan, P. (2009). Closing the peroxy acetyl nitrate budget: observations of acyl peroxy nitrates (PAN, PPN, and MPAN) during BEARPEX 2007. *Atmos. Chem. Phys.* 9: 7623–7641.

Lee, G., Jang, Y., Lee, H., Han, J.S., Kim, K.R. and Lee, M. (2008). Characteristic behavior of peroxyacetyl nitrate (PAN) in Seoul megacity, Korea. *Chemosphere* 73: 619–628.

Lee, G., Choi, H.S., Lee, T., Choi, J., Park, J.S. and Ahn, J.Y. (2012). Variations of regional background peroxyacetyl nitrate in marine boundary layer over Baengyeong Island, South Korea. *Atmos. Environ.* 61: 533–541.

Lee, J.D., Lewis, A.C., Monks, P.S., Jacob, M., Hamilton, J.F., Hopkins, J.R., Watson, N.M., Saxton, J.E., Ennis, C. and Carpenter, L.J. (2006). Ozone photochemistry and elevated isoprene during the UK heatwave of August 2003. *Atmos. Environ.* 40: 7598–7613.

Lonneman, W.A., Bufalini, J.J. and Seila, R.L. (1976). Pan and oxidant measurement in ambient atmospheres. *Environ. Sci. Technol.* 10: 374–380.

Marley, N.A., Gaffney, J.S., White, R.V., Rodriguez-Cuadra, L., Herndon, S.E., Dunlea, E., Volkamer, R.M., Molina, L.T. and Molina, M.J. (2004). Fast gas chromatography with luminol chemiluminescence detection for the simultaneous determination of nitrogen dioxide and peroxyacetyl nitrate in the atmosphere. *Rev. Sci. Instrum.* 75: 4595–4605.

Matsumoto, J. (2014). Measuring biogenic volatile organic compounds (BVOcs) from vegetation in terms of ozone reactivity. *Aerosol Air Qual. Res.* 14: 197–206.

MOE (2011). *Environmental statistics monthbook 2011*, Ministry of Environment, R.o.K. (Ed.), pp. 1–72.

Nielsen, T., Samuelsson, U., Grennfelt, P. and Thomsen, E.L. (1981). Peroxyacetyl nitrate in long-range transported polluted air. *Nature* 293: 553–555.

Phillips, G., Pouvesle, N., Thieser, J., Schuster, G., Axinte, R., Fischer, H., Williams, J., Lelieveld, J. and Crowley, J. (2013). Peroxyacetyl nitrate (PAN) and peroxyacetic acid (PAA) measurements by iodide chemical ionisation mass spectrometry: First analysis of results in the boreal forest and implications for the measurement of PAN fluxes. *Atmos. Chem. Phys.* 13: 1129–1139.

Ran, L., Zhao, C., Xu, W., Lu, X., Han, M., Lin, W., Yan, P., Xu, X., Deng, Z. and Ma, N. (2011). VOC reactivity and its effect on ozone production during the HaChi summer campaign. *Atmos. Chem. Phys.* 11: 4657–4667.

Roelofs, G.J., Lelieveld, J., Smit, H.G. and Kley, D. (1997). Ozone production and transports in the tropical atlantic region during the biomass burning season. *J. Geophys. Res.* 102: 10637–10651.

Schrimpf, W., Müller, K., Johnen, F., Lienaerts, K. and Rudolph, J. (1995). An optimized method for airborne peroxyacetyl nitrate (PAN) measurements. *J. Atmos. Chem.* 22: 303–317.

Shilling, J.E., Zaveri, R.A., Fast, J.D., Kleinman, L.,

Alexander, M., Canagaratna, M.R., Fortner, E., Hubbe, J.M., Jayne, J.T. and Sedlacek, A. (2013). Enhanced SOA formation from mixed anthropogenic and biogenic emissions during the CARES campaign. *Atmos. Chem. Phys.* 13: 2091–2113.

Sindelarova, K., Granier, C., Bouarar, I., Guenther, A., Tilmes, S., Stavrakou, T., Müller, J.F., Kuhn, U., Stefani, P. and Knorr, W. (2014). Global data set of biogenic VOC emissions calculated by the MEGAN model over the last 30 years. *Atmos. Chem. Phys.* 14: 9317–9341.

Singh, H.B. and Hanst, P.L. (1981). Peroxyacetyl nitrate (PAN) in the unpolluted atmosphere: An important reservoir for nitrogen oxides. *Geophys. Res. Lett.* 8: 941–944.

Slusher, D.L., Huey, L.G., Tanner, D.J., Flocke, F.M. and Roberts, J.M. (2004). A thermal dissociation–chemical ionization mass spectrometry (TD-CIMS) technique for the simultaneous measurement of peroxyacyl nitrates and dinitrogen pentoxide. *J. Geophys. Res.* 109: D19315.

Sobanski, N., Thieser, J., Schuladen, J., Sauvage, C., Song, W., Williams, J., Lelieveld, J. and Crowley, J.N. (2017). Day and night-time formation of organic nitrates at a forested mountain site in south-west Germany. *Atmos. Chem. Phys.* 17: 4115–4130.

Taylor, O. (1969). Importance of peroxyacetyl nitrate (PAN) as a phytotoxic air pollutant. *J. Air Pollu. Control Assoc.* 19: 347–351.

Teklemariam, T. and Sparks, J. (2004). Gaseous fluxes of peroxyacetyl nitrate (PAN) into plant leaves. *Plant Cell Environ.* 27: 1149–1158.

Thornberry, T., Carroll, M.A., Keeler, G.J., Sillman, S., Bertman, S.B., Pippin, M.R., Ostling, K., Grossenbacher, J.W., Shepson, P.B. and Cooper, O.R. (2001). Observations of reactive oxidized nitrogen and speciation of NO_y during the prophet summer 1998 intensive. *J. Geophys. Res.* 106: 24359–24386.

Tsalkani, N., Perros, P. and Toupance, G. (1987). High PAN concentrations during nonsummer periods: A study of two episodes in creteil (Paris), France. *J. Atmos. Chem.* 5: 291–299.

Tuazon, E.C., Winer, A.M. and Pitts, J.N. (1981). Trace pollutant concentrations in a multiday smog episode in the California south coast air basin by long path length fourier transform infrared spectroscopy. *Environ. Sci. Technol.* 15: 1232–1237.

Tuncay, Ö., Dinçer, A., Kuştarcı, A., Er, Ö., Dinç, G. and Demirbuga, S. (2015). Effects of ozone and photo-activated disinfection against Enterococcus faecalis biofilms in vitro. *Nige. J. Clin. Pract.* 18: 814–818.

Wang, B., Shao, M., Roberts, J.M., Yang, G., Yang, F., Hu, M., Zeng, L., Zhang, Y. and Zhang, J. (2010). Ground-based on-line measurements of peroxyacetyl nitrate (PAN) and peroxypropionyl nitrate (PPN) in the Pearl River Delta, China. *Int. J. Environ. Anal. Chem.* 90: 548–559.

Wang, Y. (2014). MeteoInfo: GIS software for meteorological data visualization and analysis. *Meteorol. Appl.* 21: 360–368.

Went, F.W. (1960). Blue hazes in the atmosphere. *Nature* 187: 641–643.

Wunderli, S. and Gehrig, R. (1991). Influence of temperature of formation and stability of surface pan and ozone. A two year field study in Switzerland. *Atmos. Environ.* 25: 1599–1608.

Xu, Z., Xue, L., Wang, T., Xia, T., Gao, Y., Louie, P.K. and Luk, C.W. (2015). Measurements of peroxyacetyl nitrate at a background site in the Pearl River Delta region: Production efficiency and regional transport. *Aerosol Air Qual. Res.* 15: 833–841.

Zhang, B., Zhao, B., Zuo, P., Huang, Z. and Zhang, J. (2017). Ambient peroxyacyl nitrate concentration and regional transportation in Beijing. *Atmos. Environ.* 166: 543–550.

Zhang, J., Wang, T., Ding, A., Zhou, X., Xue, L., Poon, C., Wu, W., Gao, J., Zuo, H. and Chen, J. (2009). Continuous measurement of peroxyacetyl nitrate (PAN) in suburban and remote areas of western China. *Atmos. Environ.* 43: 228–237.

Received for review, November 28, 2017
Revised, March 22, 2018
Accepted, April 19, 2018